Appl Water Sci (2017) 7:1827–1839
DOI 10.1007/s13201-015-0356-1

ORIGINAL ARTICLE

Site-specific functionalization for chemical speciation of Cr(III) and Cr(VI) using polyaniline impregnated nanocellulose composite: equilibrium, kinetic, and thermodynamic modeling

Priyanka Jain[1] · Shilpa Varshney[1] · Shalini Srivastava[1]

Received: 15 September 2015 / Accepted: 8 October 2015 / Published online: 22 October 2015

Abstract Site-specific functionalizations are the emergent attention for the enhancement of sorption latent of heavy metals. Limited chemistry has been applied for the fabrication of diafunctionalized materials having potential to tether both environmentally stable oxidation states of chromium (Cr(III) and Cr(VI). Polyaniline impregnated nanocellulose composite (PANI-NCC) has been fabricated using click chemistry and explored for the removal of Cr(III) and Cr(VI) from hydrological environment. The structure, stability, morphology, particle size, surface area, hydrophilicity, and porosity of fabricated PANI-NCC were characterized comprehensively using analytical techniques and mathematical tools. The maximum sorption performance of PANI-NCC was procured for (Cr(III): 47.06 mg g^{-1}; 94.12 %) and (Cr(VI): 48.92 mg g^{-1}; 97.84 %) by equilibrating 0.5 g sorbent dose with 1000 mL of 25 mg L^{-1} chromium conc. at pH 6.5 and 2.5 for Cr(III) and Cr(VI), respectively. The sorption data showed a best fit to the Langmuir isotherm and pseudo-second-order kinetic model. The negative value of $\Delta G°$ (-8.59 and -11.16 kJ mol^{-1}) and $\Delta H°$ (66.46 × 10^{-1} and 17.84 × 10^{-1} kJ mol^{-1}), and positive value of $\Delta S°$ (26.66 and 31.46 J $mol^{-1}K^{-1}$) for Cr(III) and Cr(VI), respectively, reflect the spontaneous, feasibility, and exothermic nature of the sorption process. The application of fabricated PANI-NCC for removing both the forms of chromium in the presence of other heavy metals was also tested at laboratory and industrial waste water regime. These findings open up new avenues in the row of high performance, scalable, and economic nanobiomaterial for the remediation of both forms of chromium from water streams.

Keywords Site-specific functionalization · Click reaction · Cr(III) and Cr(VI) remediation · Waste water treatment

Introduction

The last few decades have seen enormous growth in the chemical functionalization onto biomaterial for the binding of either cationic or anionic heavy metals. Biomaterials functionalized with different chemical agents explored for the abatement of heavy metals are listed in Table 1. However, these biomaterials possess toxicity issue, low sorption performance, slow removal rate, and low reusability (Jain et al. 2003; Gupta and Nayak 2012; Qiu et al. 2015; Akhavan et al. 2015) and do not have aptitude to remove both cationic and anionic forms of heavy metals. Such functionalized biomaterials are proved to be idealistic but impracticable in commercialization. From the ken of literature, it is apparent that little efforts have been made toward the fortification of amphoteric natured functionalization that contains cationic and anionic functionalities.

In this conception, we sought to pave the attention toward such type of functionalization which has the talent to significantly tether the both cationic and anionic heavy metals via simple and green process. Of the known ways of functionalization, click reaction is one of the most artistic green approaches for the tailoring of biomaterials (Filpponen et al. 2012; Navarro et al. 2015). To meet out the desired requirement, polyaniline (PANI) is remarkably recognized as diafunctional green polymer having amine (:NH_2) and imine (NH^+) functionalities (Wang et al. 2014;

✉ Shalini Srivastava
dei.shalinisrivastava@gmail.com

[1] Department of Chemistry, Faculty of Science, Dayalbagh Educational Institute, Agra 282 005, India

Table 1 Summary of different chemical functionalizations onto biomaterials for heavy metal remediation

S. no.	Functionalized nanocellulose	Heavy metal remediation	Maximum sorption performance (mg/g)	References
1.	Cellulose bead-acrylonitrile	Cr(III)	7.50	Liu et al. 2002
2.	Succinic anhydride + triethylenetetramine modified cellulose	Cr(VI)	43.09	Gurgel et al. 2009
3.	Amino-functionalized magnetic cellulose composite	Cr(VI)	17.56	Yang et al. 2011
4.	Poly (methacrylic acid)	Cu(II)	2.8	Tian et al. 2011
		Hg(II)	3.4	
		Cd(II)	4.2	
5.	Cellulose-montmorillonite	Cr(VI)	22.20	Kumar et al. 2012
6.	Glycidyl methacrylate + aminated cellulose	Cr(VI)	12.61	Anirudhan et al. 2013
7.	Succinated & aminated nanocellulose	Cr(III)	10.21	Singh et al. 2014
		Cr(VI)	11.84	
8.	Polyethylenimine facilitated ethyl cellulose	Cr(VI)	36.87	Qiu et al. 2014
9.	Polyacrylamide zirconium(IV) iodate	Pb(II)	5.98	Rahman and Haseen 2014
10.	Polyaniline impregnated nanocellulose	Cr(III)	47.06	Present work
		Cr(VI)	48.92	

Fumagalli et al. 2015). This motivates the impregnation of diafunctionalized polyaniline onto biomaterial for taking the advantages of amine and imines functional groups for the effective removal of cationic Cr(III) and anionic Cr(VI).

Among all the natural biomaterials that are used for functionalization, cellulose is the foremost structural cog of plants and contemporary strive for sustainable environment and has remunerated scientific interest for heavy metals remediation, particularly in the form nanocellulose (NC). NC is a quintessence of nanomaterials attesting to incredible physical and chemical attributes which formulate them highly lucrative as a nanosorbent because of larger surface area, high crystallinity, renewability, and sustainability (Gardner et al. 2008; Srivastava et al. 2012; Xue et al. 2015). Indeed, attendance of prodigious hydroxyl groups within their structure which can offer suitable platform for functionalization (Klemm et al. 2011; Wei et al. 2014). In this reason, scientists and researchers have recently employed as a template material.

In this article, we report a fabrication of polyaniline impregnated nanocellulose composite (PANI-NCC) from pristine cellulose using click chemistry reaction for the remediation of both Cr(III) and Cr(VI) as a model heavy metal from hydrological environment. Exploration of the sorption performance of PANI-NCC for propitious remediation of chromium in non-competitive and competitive environment has been carried out in the attendance of heavy metals like Ni(II), Cd(II), and Pb(II) at laboratory regime. The equilibrium, kinetic, and thermodynamic models were studied to decipher mechanistic aspects for sorption. To comprehend the fecundity of PANI-NCC, its sorption potential was tested to industrial chrome tannery effluent.

Materials and methods

Preparation of nanocellulose (NC)

NC was synthesized from cellulose from previously reported protocol (Ghahafarrokhi et al. 2015) with minor modifications. Briefly, cellulose (50.0 g, ACS chemicals; our industry research collaborator) was dissolved in water and cooled for 10 min in an ice bath. Then, sulfuric acid (54 %, w/v) was slowly added keeping the temperature below 20 °C and stirred magnetically at 45 °C for 3 h. The reaction was stopped by pouring water and cooled in an ice bath. The NC was purified by centrifugation (2500 rpm/15 min). The supernatant was decanted and replaced by an equal amount of water, and the mixture was centrifuged again. The purification steps were repeated for five times. The NC thus obtained was dialyzed against water for 7 days, exchanging the water every day, until the pH was neutral. Thereafter, NC was sonicated for 15 min and finally dried at ambient temperature. The yield of NC thus isolated was 80–85 %. These benchmark conditions were selected to significantly boom the yield of NC. Ultrapure water was used throughout the study.

Assessment of surface hydroxyl groups of NC for functionalization

NC possesses copious surface hydroxyl groups which offer apposite for functionalization. The content of surface hydroxyl groups of NC was calculated using mathematical equation:

$$n_{OH} = \left(\frac{N_1 N_2}{N_A}\right) = 3\left(\frac{w}{\rho_{CN} V_{CN}}\right)\left(\frac{S_{CN}}{S'}\right)\frac{1}{N_A}$$

where

$$N_1 = \left(\frac{w}{\rho_{CN}}\right)\Big/ V_{CN}$$

$$N_2 = 3\left(\frac{S_{CN}}{S'}\right)$$

$$V_{CN} = \pi\left(\frac{d}{2}\right)^2 L$$

$$S_{CN} = \pi dL + \pi\left(\frac{d}{2}\right)^2 \approx \pi dL$$

$$S' = d'L'$$

where N_1 allocates the number of NC crystals, N_2 corresponds the number of hydroxyl groups on an individual NC crystal, N_A (6.02×10^{23} mol^{-1}) represents Avogadro number, V_{CN} corresponds to the volume of NC crystal, S_{CN} is related to the surface area of individual NC crystal, and S' is the surface area of two glucose units. The density (ρ_{CN}), width (d'), and length (L') of two glucose units of 1.0 g NC are constant, which are 1.606 g cm^{-3}, 0.79, and 1.03 nm, respectively (Lin et al. 2012). The average width (d) and average length (L) were computed by PSD and XRD analysis, respectively.

Fabrication of polyaniline impregnated nanocellulose composite (PANI-NCC)

For the fabrication of PANI-NCC, aniline (7.5 mL, Fischer scientific) was dissolved in conc. HCl (60 mL; 1 M, Merck). Thereafter, reaction mixture was charged with ammonium persulfate solution (2 g in HCl 15 mL; 1 M) followed by stirring for 16 h. From the above prepared polyaniline, 50 mL was taken and mixed with NC (10 g) with further stirring for another 10 h. After centrifuged at 2500 rpm, the obtained insoluble dark-green precipitate was washed with ultrapure water until water became colorless. Subsequently, the obtained PANI-NCC was washed with ethanol (99 %, Fischer scientific), then sonicated, and finally dried at ambient temperature. The quantitative estimation of amine functionalities was attained by volumetric method according to the procedure presented previously (Donia et al. 2012).

Water regain factor

Water regain factor (W%) is linked to the hydrophilic and hydrophobic nature of the sorbents using gravimetric method (Elwakeel 2009). Briefly, PANI-NCC (0.5 g) was put into a weighed polypropylene bag and immersed in ultrapure water (100 mL) for 40 min and then weighed. Thereafter, PANI-NCC was then dried at 50 °C until complete dryness then weighed again. The aforementioned nature of PANI-NCC was investigated using mathematical expression:

$$W\% = \frac{100\,(W_w - W_d)}{W_w}$$

where W_w and W_d are the weights (g) of wet and dried PANI-NCC.

Testing of sorption performance

Chromium containing wastewater was primed by diluting ultrapure water with doses of chromium chloride hexahydrate ($CrCl_3.6H_2O$, Merck) for Cr(III) and potassium dichromate ($K_2Cr_2O_7$, Merck) for Cr(VI), resulting in solutions at environmentally relevant concentrations which are in the order of 5–30 mg L^{-1}. The sorption performance of fabricated PANI-NCC for chromium remediation in non-competitive environment was investigated in batch assays as a function of kinetic time (10–60 min), sorbent dosage (0.1–1.0 g), chromium concentration (5–30 mg L^{-1}) and solution pH (2.5–7.5) at sample volume (1000 mL). The solution pH was deliberated by employing a digital pen type pH-meter and adjusted with HCl (0.1 M, Merck) or NaOH (0.1 M, Merck). After that, a known amount of PANI-NCC was added at 350 rpm stirring for better mass transport with high interfacial area of contact. After that, chromium laden PANI-NCC was filtered, and the filtrate was subjected for chromium ions analysis using atomic absorption spectrophotometer (AAS analyst-100, Perkin–Elmer) at resonance wavelength 357.9 nm. During experiments, we tested the solution pH before and after sorption and found that pH varied $\sim$0.1, so influence could be neglected.

The sorption performance of PANI-NCC was also tested in competitive environment in the mixture of Cd(II), Ni(II), Pb(II), and Cr(III) and Cr(VI) ions at optimum conditions for the investigation of the practical utility of PANI-NCC from real hydrological environment. Cd(II), Ni(II), and Pb(II) were analyzed in the same way as chromium ions. The sorption performance was calculated by equation:

$$\text{Sorption percentage} = \frac{(C_0 - C_e)}{C_0} \times 100$$

$$Q_e\left(\text{mg g}^{-1}\right) = \left[\frac{(C_0 - C_e)V}{m}\right]$$

where C_0 and C_e(mg L^{-1}) are the initial and final concentrations, m (g) is the amount of the PANI-NCC, and V (mL) is the sample volume. For statistical soundness, data shown here were the mean of triplicate trials with error less than 5 %. The reusability of PANI-NCC was achieved by (1 M NaOH). Such adsorption–desorption process was repeated six times.

Characterization

FTIR measurements were recorded using Cary 630 FTIR with a resolution of 4 cm^{-1} and a scanning number of 64 from 4000 to 700 cm^{-1} range in transmittance mode. The energy-dispersive X-ray spectroscopy (EDX) analysis of PANI-NCC was examined with LECO TruSpec CHN analyzer. Thermogravimetric analyses (TGA) were performed with a TG instrument (Q500 V6.3, 189) heated from temperature 200 to 1300 K at the rate of 298 K min^{-1} under nitrogen atmosphere. The powder X-ray diffraction (XRD) analyses were acquired using Bruker AXS D8 Advance X-ray diffractometer, Germany with Cu-Kα radiation source filtered (λ = 1.5406 Å) at 40 kV and 30 mA. The 2θ angle was stepped from 5° to 40° at scan rate of 2° min^{-1}. Particle size analysis was done using a Zeta sizer NanoZS instrument (Malvern, UK). Three measurements of 10 s each were taken for averaging. The nitrogen sorption–desorption isotherm was recorded using micromeritics ASAP 2020 analyzer.

Results and discussion

Characterization of fabricated PANI-NCC

In the present work, PANI-NCC was fabricated using pristine cellulose, as a starting material. The fabrication of PANI-NCC that included a two-step process is depicted in Fig. 1a. Firstly, pristine cellulose was converted into NC by the protonation of glucosidic oxygen centers, attacked by protons of sulfuric acid. Subsequently, breakage of glucosidic bonds was induced by the water. During this process, two new-fangled hydroxyl groups per two glucose units are formed with preserving the pristine cellulose structure, as shown in Fig. 1b. The quantitative increment

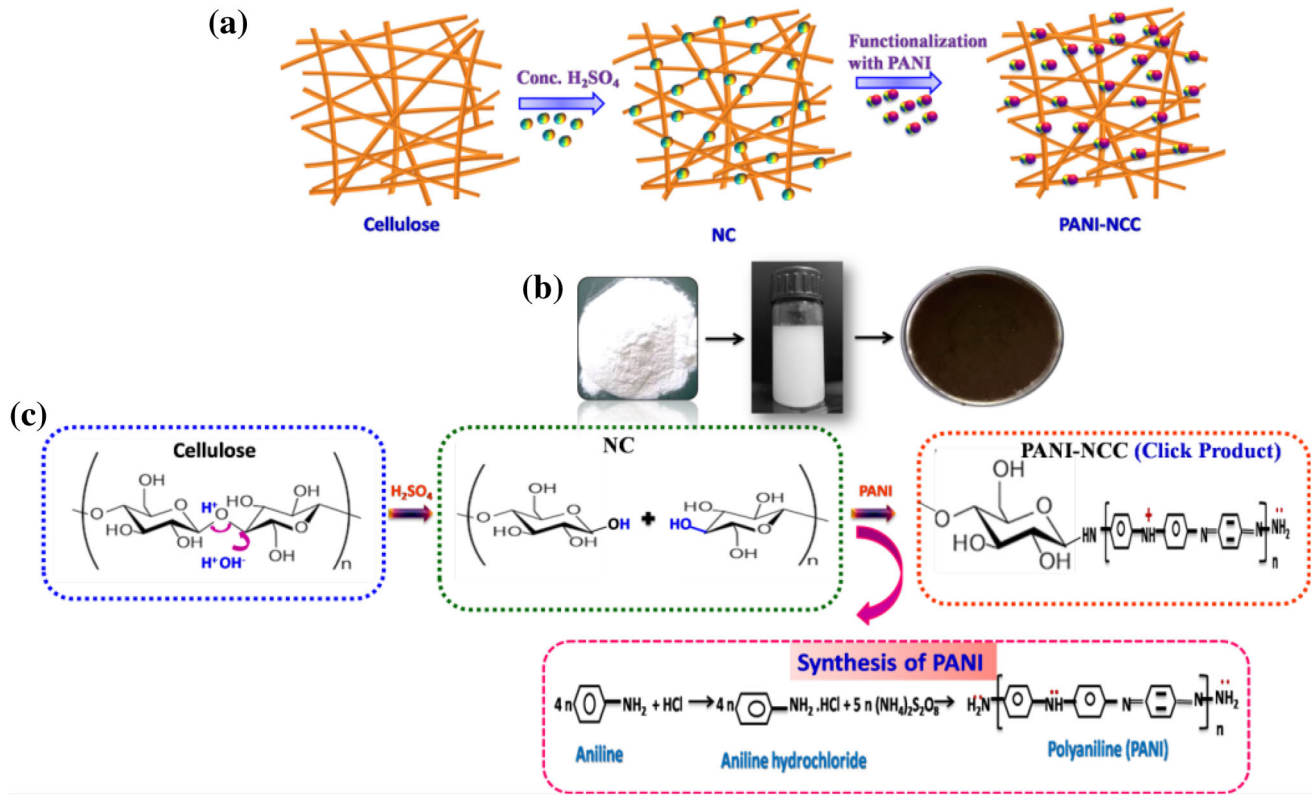

Fig. 1 **a** Schematic illustration for the fabrication of PANI-NCC (Click product), **b** photographs showing the morphological and *color* changes during the fabrication of PANI-NCC, **c** Chemical route and structure of NC and PANI-NCC by using click reaction

of surface hydroxyl groups onto NC was computed by mathematical tool and found to be 2.6 mmol g^{-1}.

Secondly, PANI was impregnated on NC via click chemistry route performing between surface hydroxyl groups of NC and :NH_2 groups of PANI. During fabrication of nanocomposite, there was no side product with high atom economy (89 %), representing that synthetic route follows the doctrine of click chemistry reactions.

Confirmation for the fabrication of PANI-NCC was examined by FTIR. As is obvious from Fig. 2a, strong bands at 3320, 2895, 1652, 1437, and 1020 cm^{-1} are ascribed to O–H (stretching vibration), C–H (stretching vibration), O–H (bending vibration), C–H (bending vibration), and C–O (stretching vibration) groups, respectively (Zhang et al. 2012). These peaks are all the characteristic absorption bands of cellulose. Notably, we observed that, in the FTIR spectrum of NC, the O–H stretching band is shifted toward lower wave number (blue shifted) and become higher intense (hyper chromic) as endowed in Fig. 2a, confirming that during NC preparation, breakage of glucosidic bonds took place in pristine cellulose structure (Benkaddour et al. 2013). This result evinces the successful preparation of NC.

In FTIR spectrum of fabricated PANI-NCC (Fig. 2a), new bands appeared at 1530 and 1458 cm^{-1} with equal intensity (Fig. 2b) are linked to C=N (stretching vibration) of quinonoid ring and C=C (stretching vibration) of benzenoid ring, respectively, while band at 1265 cm^{-1} is allied to C=N (stretching vibration) of secondary amine (Shyaa et al. 2015), demonstrating the attendance of amine functionalities on the surface of PANI-NCC. Furthermore, the quantitative estimation amine functionalities were determined by volumetric method and found to be 8.9 mmol g^{-1}. These results confirm the facile fabrication of PANI-NCC.

Further confirmation of fabrication of PANI-NCC was clarified by EDX analysis. As shown in Fig. 3a, the attainment of nitrogen peak in the spectra endowed the impregnation of PANI onto NC.

Furthermore, TGA was used to further prove the fabrication of PANI-NCC. As revealed from Fig. 3b, the onset degradation temperature at which maximum weight loss of pristine cellulose, NC, and PANI-NCC was occurred at 554, 600, and 646 K, respectively. The thermal behavior and decrement in weight loss are due to the breakage of cellulose chains and evolution of non-combustible gases such as CO_2, CO, HCOOH, and CH_3COOH. TG curve noticeably shows that PANI-NCC has higher onset degradation temperature (646 K) than that of pristine cellulose and NC, relying that PANI-NCC is more stable (Espinosa et al. 2013; Li et al. 2014) which is due to the presence of thermally stable amine functional groups.

The hydrophilic behavior of PANI-NCC was ascertained by water regain factor. The value of water regain factor was computed in the order of 56 ± 2 %, suggestive of hydrophilic nature of PANI-NCC, owing to the presence of hydrophilic functionalities (:NH_2 and NH^+) onto the surface of PANI-NCC.

The particle size, surface area, and pore size took play an imperative role in sorption process. In this conception, the particle size was ascertained by XRD analysis. The XRD spectra of pristine cellulose, NC, and PANI-NCC are

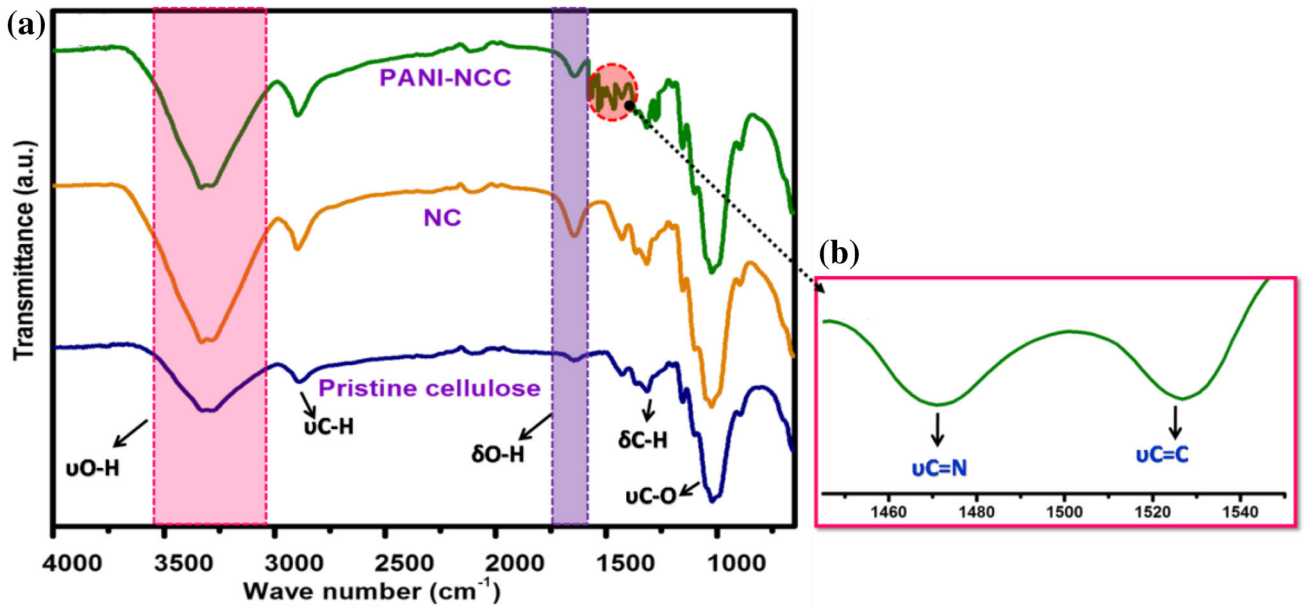

Fig. 2 **a** FTIR spectra of pristine cellulose, NC, and PANI-NCC, **b** FTIR spectra showing the presence of equally intense bands in PANI-NCC

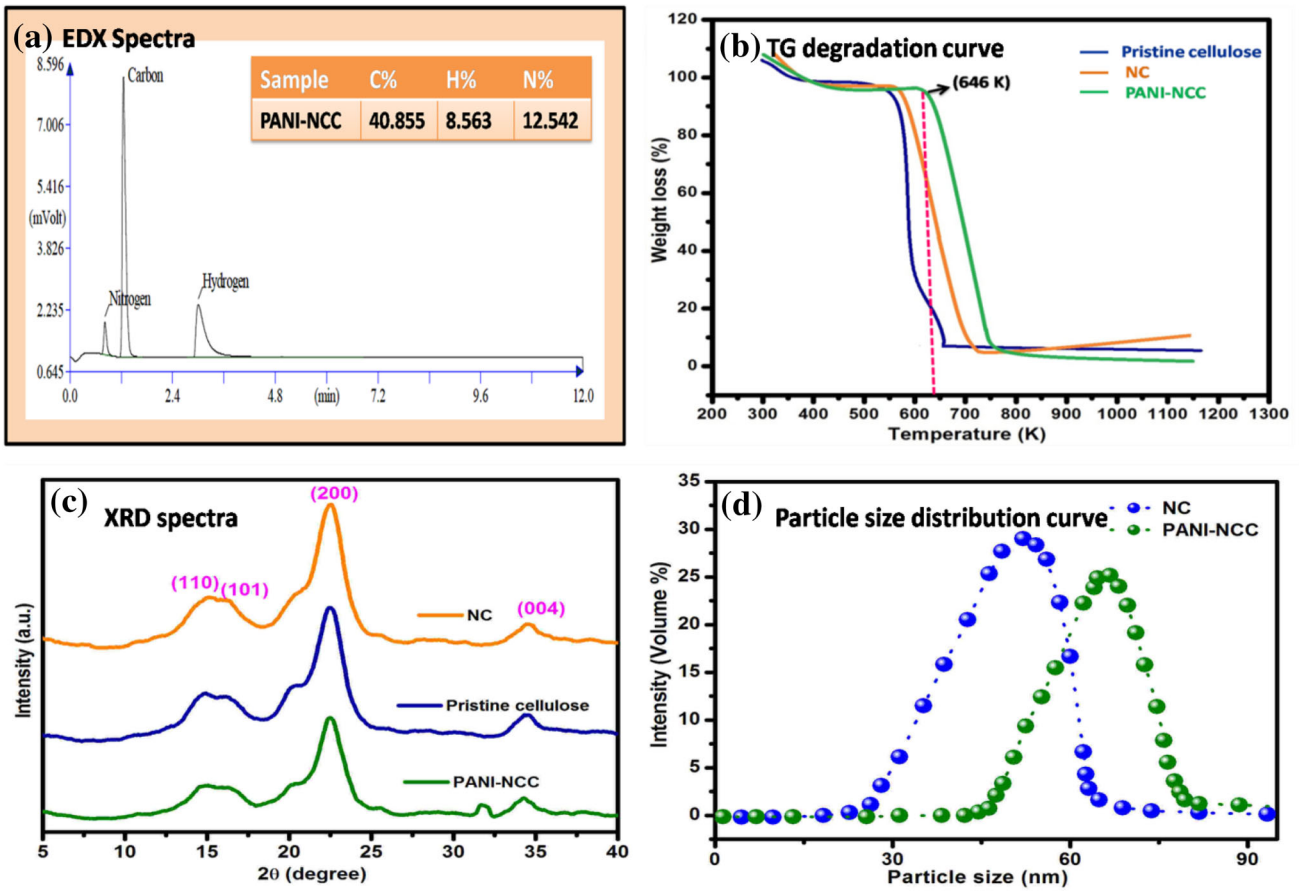

Fig. 3 **a** EDX spectra of PANI-NCC, **b** Thermal degradation curves of pristine cellulose, NC, and PANI-NCC, **c** XRD spectra of pristine cellulose, NC, and PANI-NCC, **d** Particle size distribution curve of PANI-NCC

presented in Fig. 3c. We can find that all the diffraction maxima at $2\Theta = 15.9°$ (d_{110}), 22.6° (d_{200}) and 34.6° (d_{004}) show a similar XRD pattern which is a characteristic pattern of pristine cellulose as in accordance with JCPDS card no. 00-050-2241 (Lu and Hsieh 2010), while the XRD pattern of PANI-NCC endows new peak at 31.59° is indexed to nitrogen as indicated by JCPDS data (card no. 00-023-1292), demonstrating that existence of amine functionalities on the surface of PANI-NCC. In addition, the average particle size of PANI-NCC was estimated from the full width at half-maximum intensity (FWHM) using Debye–Scherrer equation.

$$\beta_{hkl} = \frac{K\lambda}{L_{hkl}} \cos\theta_{hkl}$$

where β is the breadth of diffraction maxima at $2\theta = 22.51$, K (0.94) is the constant, λ (0.15418 nm) is the wavelength of incident X-rays, θ is the diffraction angle, and L is the crystalline length, and particle size of PANI-NCC was found to be ~60 nm. Furthermore, crystallinity index (CI%) of PANI-NCC was ascertained from the heights of the 200 peak (I_{200}) and the intensity of minimum between the 200 and 110 peaks using Buschle-Diller and Zeronian equation:

$$I_{200} - I_{101}/I_{200} \times 100$$

with an error of 0.8 % and calculated to be 84.18 %. Furthermore, judgment of particle size was examined by particle size analyzer. As shown in Fig. 3d, the particle size of PANI-NCC was found to be 60–70 nm, supporting the result of XRD.

The surface area, pore size, and pore volume of PANI-NCC were investigated using nitrogen sorption–desorption isotherm. The surface area was computed by Brunauer–Emmett–Teller (BET) method, and pore size was determined by Barret–Joyner–Halenda (BJH) method. As is obvious from Fig. 4a, the isotherm is related with the characteristic of type IV isotherm with a type H_3 hysteresis, representing that PANI-NCC is mesoporous in nature (Zargoosh et al. 2013; Gu et al. 2015). The surface area of PANI-NCC was found to be 112.26 $m^2\ g^{-1}$. As shown in Fig. 4b, the pore size distribution curve of PANI-NCC provides a pore size in the range of 2-5 nm at maximum pore volume of 0.28 $cm^3\ g^{-1}$.

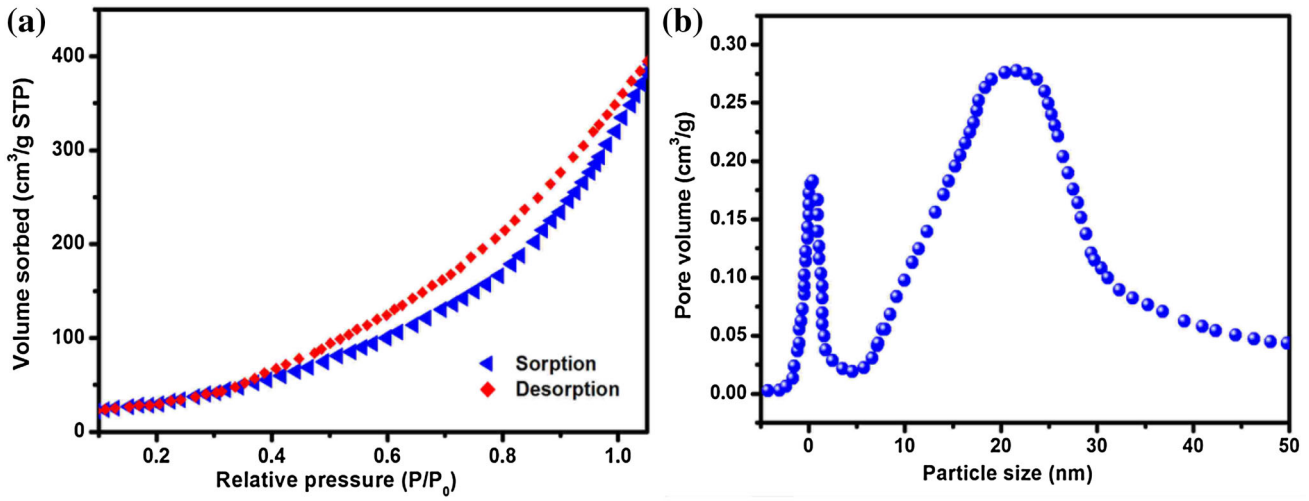

Fig. 4 **a** Nitrogen sorption–desorption isotherm, **b** pore size distribution curve of PANI-NCC

Effect of solution pH

The solution pH is the vital parameter administers the rate of sorption of metals onto materials as it influences both the chemistry of functionalities plus the solution chemistry of chromium ions. The effect of solution pH is displayed in Fig. 5. It can be observed that Cr(III) sorption occurs under basic pH conditions and uptake of Cr(III) speedily increases with the increase in solution pH and attainment of maximum uptake at 6.5. Within the pH range studied from 2.5 to 6.5, the removal of Cr(III) is solely due to the sorption as no precipitation was detected. Similarly, maximum Cr(VI) sorption occurs at acidic pH (2.5). The corresponding photographs displayed that the color of chromium solutions was changed to colorless after sorption, see in the inset of Fig. 5.

At low solution pH, the functionalities onto PANI-NCC are protonated and formed positive surface charge (NH^+).

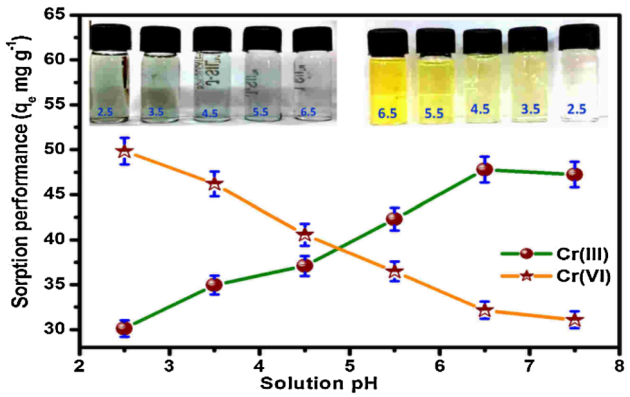

Fig. 5 Effect of solution pH on the sorption of Cr(III) and Cr(VI) conditions: (0.5 g PANI-NCC; 25 mg L^{-1} chromium conc.; 1000 mL sample volume; pH (6.5 for Cr(III) and 2.5 for Cr(VI)) and 298 K temperature)

This induces the electrostatic attraction between the positively charged NH^+ and the free anionic Cr(VI). Moreover, when the solution pH increases up to 6.5, the functionalities onto PANI-NCC are deprotonated forming negative charge surface (:NH_2) and capable to sorb cationic Cr(III) through electrostatic attraction. This can be explained by the different positions of the point of zero charge (PZC) of PANI-NCC. The pH at PZC (pH_{PZC}) defines the Coulombic interactions between the surface of functionalized nanomaterials and chromium species. Since the surface of PANI-NCC is positively charged at pH of solution is lower than pH PZC (pH of point of zero charge of PANI-NCC) and it becomes negatively charged when pH of solution is greater than pH PZC (Chingombe et al. 2005; Saleh and Gupta 2012a; Dichiara et al. 2015). This is the reason maximum uptake of cationic Cr(III) at basic pH and anionic Cr(VI) at acidic pH. These results are consistent with previous studies reporting the sorption of metal ions (Mittal et al. 2010b; Anirudhan and Rejeena 2012; Hokkanen et al. 2013; Gupta et al. 2013). Therefore, PANI-NCC has an ability to sorb both cationic and anionic metals by changing the pH conditions.

Sorption isotherm

The mechanistic aspects of interactions between sorbent and sorbate at equilibrium were fundamentally explained by using Langmuir isotherm model. The Langmuir model is anchored in the assumption that a fixed number of sorption sites is presented on the sorbent surface, and each site can occupy a maximum of one molecule at sorption energy that becomes constant. Prior applying the model, the effect of the chromium concentration on the sorption performances was studied which is shown in Fig. 6a. From this, the equilibrium concentration was determined for

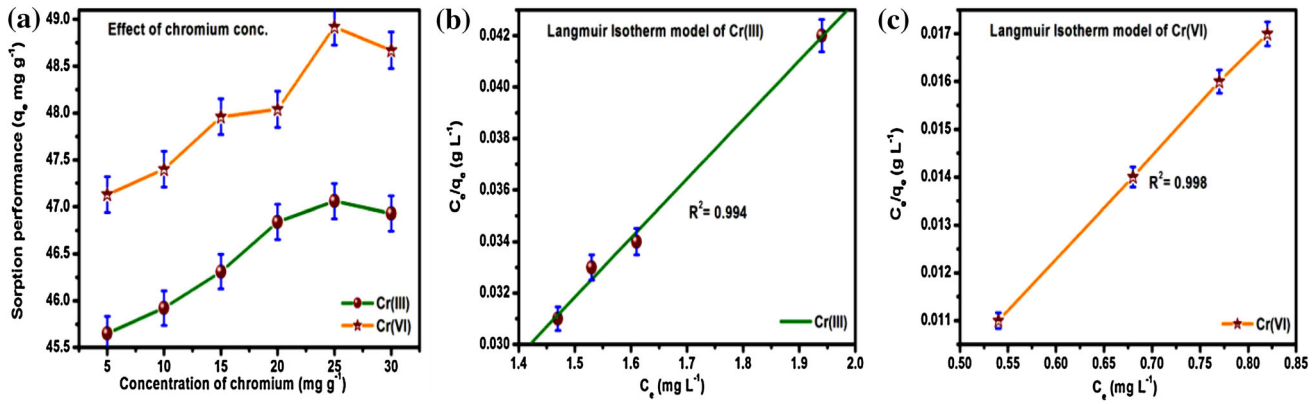

Fig. 6 **a** Effect of concentration of chromium, **b** Langmuir isotherm model of Cr(III), **c** Langmuir isotherm model of Cr(VI) conditions: (0.5 g sorbent dose; 25 mg L^{-1} chromium conc.; 1000 mL sample volume; pH (6.5 for Cr(III) and 2.5 for Cr(VI)) and 298 K temperature)

Table 2 Langmuir isotherm, pseudo-second order and intraparticle diffusion model parameters for Cr(III) and Cr(VI)

Chromium ion	q_e (exp) (mg g^{-1})	Langmuir Isotherm model			Pseudo-second order		Intraparticle diffusion model	
		q_m (mg g^{-1})	b (L mg^{-1})	R_L	k_2 (g mg^{-1} min^{-1})	q_e (cal) (mg g^{-1})	K_i (mg g^{-1} min^{-1})	C (mg g^{-1})
Cr(III)	47.06	55.55	0.62	0.06	3.41×10^{-3}	47.62	2.51×10^{-1}	46.21
Cr(VI)	48.92	47.17	2.16	0.02	3.10×10^{-3}	50.00	2.39×10^{-1}	48.30

Exp experimental result, *cal* calculated result

Langmuir isotherm model. The Langmuir equation is defined as follows:

$$\frac{C_e}{q_e} = \frac{1}{bq_m} + \frac{C_e}{q_m}$$

where C_e (mg L^{-1}) and q_e (mg g^{-1}) are the residual concentration and amount of sorbed chromium at equilibrium, respectively; q_m (mg g^{-1}) is the maximum sorption capacity allied to complete monolayer coverage; and b (L mg^{-1}) is Langmuir-binding constant corresponded to sorption energy. The results are summarized in Fig. 6b, c and Table 2. As is obvious from Fig. 6b, c and Table 2, the values of correlation coefficient (R^2) attested by Langmuir model are greater than 0.99. Furthermore, the Langmuir sorption capacity is consistent with experimental values, indicative of the monolayer and homogenous uptake of chromium ions (Mittal et al. 2009a; Gupta et al. 2012a; Dhawan et al. 2015), while the large value of b specifies electrostatic binding of chromium ions onto fabricated PANI-NCC (Renault et al. 2008; Gupta et al. 2014).

The feasibility of Cr(III) and Cr(VI) sorption was determined with a dimensionless constant (R_L) known as separation factor which can be defined as

$$R_L = 1/(1 + bC_o)$$

The R_L value was used to envisage the sorption behavior to be either irreversible ($R_L = 0$), feasible ($0 < R_L < 1$), linear ($R_L = 1$) or non-feasible ($R_L > 1$). In the present study, the calculated R_L values are $0 < R_L < 1$, signifying that sorption process is feasible (Mittal et al. 2009b; Gupta et al. 2011a; Karthikeyan et al. 2012).

Sorption kinetics

The rate of sorption is one of the most fundamental attributes of the sorbent. Figure 7a shows the effect of time on the sorption of Cr(III) and Cr(VI). It is noteworthy that the Cr(III) and Cr(VI) speedily achieved equilibrium at 40 min, probing that the PANI-NCC possesses excellent sorption performance with fast sorption kinetics. This might be ascribed to higher surface area, as we have calculated above and greater availability of NH^+ and $:NH_2$ functionalities which are accessible for the sorption of Cr(III) and Cr(VI), respectively.

To understand the mechanistic aspect between surface functionalities and the chromium ions, kinetic models were conducted using pseudo-second-order model and intraparticle diffusion model, respectively.

$$\frac{t}{q_t} = \frac{1}{k_2 q_e^2} + \frac{1}{q_e} t$$

$$q_t = c + k_i t^{0.5}$$

where q_t and q_e (mg g^{-1}) represent the amount of sorbed chromium ions at time t and equilibrium time, respectively; k_2 (g mg^{-1} min^{-1}) and k_i (mg g^{-1} min^{-1}) correspond to

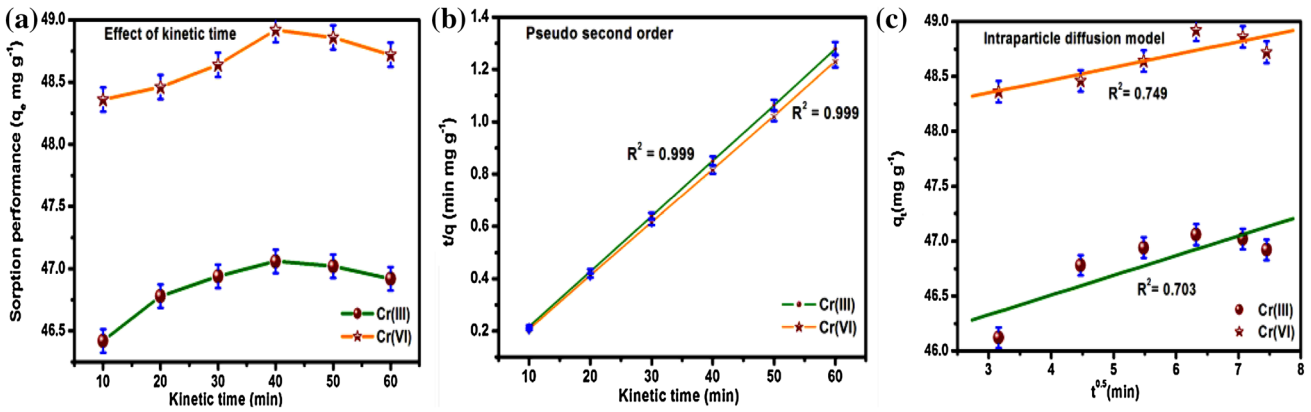

Fig. 7 **a** Effect of time on the sorption of chromium ions, **b** pseudo-second order, **c** intraparticle diffusion model (0.5 g sorbent dose; 25 mg L^{-1} chromium conc.; 1000 mL sample volume; pH (6.5 for Cr(III) and 2.5 for Cr(VI)) and 298 K temperature)

the pseudo-second order and the intraparticle diffusion rate constant, respectively; and C is the intercept. As it is noticeable from Fig. 7b, c and Table 2, we revealed that pseudo-second-order kinetic model can best elucidate the sorption process because it possessed a higher 0.99 R^2 value (Khani et al. 2010; Mittal et al. 2010a; Gupta et al. 2012b; Saleh and Gupta 2012b). These results confirmed the paramount role of electrostatic attractions in the rate-limiting step. Sorption process is chemisorption in nature (Gupta et al. 1998; Cruz et al. 2004; Gupta et al. 2004).

Sorption thermodynamics

For further confirmation of the paramount role of electrostatic attractions and the feasibility of sorption process, we studied the change in Gibb's free energy ($\Delta G°$), enthalpy ($\Delta H°$), and entropy ($\Delta S°$).

$$\Delta G^\circ = -RT \ln K_c; \quad K_c = \frac{C_{Ae}}{C_e}$$

$$\Delta H^\circ = -R\left(\frac{T_2 T_1}{T_2 - T_1}\right) \ln \frac{k_2}{k_1}$$

$$\Delta S^\circ = \frac{\Delta H^\circ - \Delta G^\circ}{T}$$

where K_c is the equilibrium constant, C_{Ae} (mg L^{-1}) is the amount of sorbed Cr(III) and Cr(VI) at equilibrium, C_e (mg L^{-1}) is the equilibrium concentration of Cr(III) and Cr(VI) in the solution, R (8.314 J/mol K) is universal gas constant, and T (K) is absolute temperature; k_1 and k_2 are equilibrium constants at temperatures T_1 and T_2. The negative value of $\Delta G°$ (−8.59 and −11.16 kJ mol^{-1} for Cr(III) and Cr(VI), respectively) and positive value of $\Delta S°$ (26.66 and 31.46 J mol^{-1} K^{-1} for Cr(III) and Cr(VI), respectively) reflect the spontaneous and feasibility of the sorption process (Gupta et al. 2001; Asem et al. 2008). Furthermore, the negative values of $\Delta H°$ for Cr(III) and Cr(VI) were obtained as 66.46 × 10^{-1} and 17.84 × 10^{-1} kJ mol^{-1}, respectively, indicative of principal role of electrostatic interactions and exothermic nature of the sorption process (Wang et al. 2010; Gupta et al. 2011b).

Sorption activation energy

The activation energy can be contemplation of the minimum energy requisite for a chemical reaction to surmount the energetic barrier that the sorbate ions could be fixed by the sorbents. The activation energy (E_a, kJ mol^{-1}) of the sorption was anticipated using equation:

$$\ln \frac{k_2}{k_1} = \frac{E_a}{R}\left(\frac{1}{T_1} - \frac{1}{T_2}\right)$$

where k_2 and k_1 (g mg^{-1} min^{-1}) are associated to pseudo-second-order rate constant at temperatures T_1 and T_2, respectively. According to the parameters of the pseudo-second-order kinetic model, activation energies of Cr(III) and Cr(VI) on PANI-NCC are calculated as 8.93 and 3.40 kJ mol^{-1}, respectively. These results indicated that the value of E_a of Cr(VI) is lower than that of Cr(III), probing that the energetic barrier against the sorption of Cr(VI) ion is easier to overcome; therefore, the sorption reaction of Cr(VI) is more facile to occur than that of Cr(III).

Sorption latent of Cr(III) and Cr(VI) in competitive environment

It is mandatory to study the competitive effect of other metal ions for the sorption latent of chromium ions. Prior applying in hydrological streams, the artificial waste water was prepared by the amalgam of Pb(II), Cd(II), Ni(II), and Cr(III) and Cr(VI) ions, containing equal initial

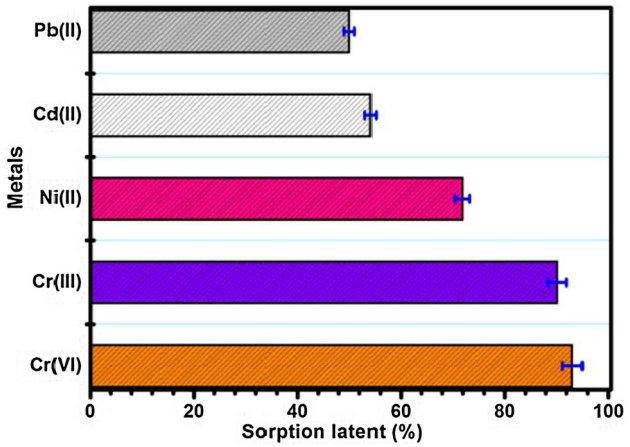

Fig. 8 Sorption latent of Cr(III) and Cr(VI) in competitive environment

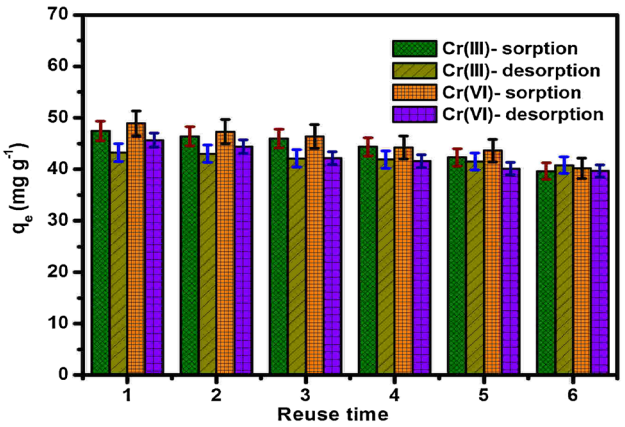

Fig. 9 Performance of PANI-NCC in reusability cycles

concentrations (25 mg L^{-1}). For testing the sorption performance, PANI-NCC (0.5 g) was added to the amalgamated solution (1000 mL). The pH was maintained at 6.5, and kinetic time was 40 min. The obtained sorption performances of studied metal ions are in the order of Cr(VI):93.10 % > Cr(III):90.19 % > Ni(II):71.92 % > Cd(II):54.12 % > Pb(II):50.03 %.

The observed differences in the sorption performance are solely due to diverse kinship of the studied metal ions with amine functionalities. According to Pearson's classification, Cr(III) and Cr(VI) are categorized as a hard acid, and amine is classified as a hard base. Notably, sorption latent of Cr(III) and Cr(VI) is higher than other metal ions as shown in Fig. 8, demonstrating that paramount role of hard–hard interaction for high sorption latent. Conversely, Ni(II) is on the borderline of the soft and hard acids, while Cd(II) and Pb(II) are soft acids. Therefore, they have lower affinity toward amine functionalities, due to the existence of hard–soft interaction. Fantastically, we prove that sorption performance of PANI-NCC is specifically for Cr(III) and Cr(VI) ions.

Reusability of PANI-NCC

The regeneration of sorbent is indispensable from a greener perspective and hence it is imperative to look for effective and non-toxic eluents for the quantitative recovery of chromium. Considering the above point in mind, eluent such as sodium hydroxide was examined for effective desorption under optimum conditions. The reagent has also proved their efficacy in some of our earlier studies pertaining to the abatement of chromium (Kalidhasan and Rajesh 2009; Kardam et al. 2012). The results are depicted in Fig. 9. As is understandable from Fig. 9, the chromium sorption performance was remained almost constant for five cycles, representing that the interactions between chromium ions and the surface functionalities of fabricated PANI-NCC are reversible. Beyond five cycles, the sorption performance was decreased due to the non-availability of active sites for further sorption.

Remediation of Cr(III) and Cr(VI) from industrial effluent

The practical utility of fabricated PANI-NCC for Cr(III) and Cr(VI) remediation was evaluated from chrome tannery leather effluent sample. At the time of collection, the chrome waste liquor was green with 6.5 pH. It is due to the presence of basic chromium sulfate, which is used in leather tanning. Prior to sorption, it is essential to devastate the organic moieties present in the effluent, and this was maintained by sulfuric acid–nitric acid amalgam. Sorption performance of PANI-NCC was tested at experimentally optimized conditions. Interestingly, we found that sorption latent of chromium in the same order as with those obtained in competitive environment. These results indicate that fabricated PANI-NCC can be used for effective removal of Cr(III) and Cr(VI) without interfering the influence of other heavy metal ions from industrial effluent and waste water.

Conclusions

In summary, PANI-NCC was successfully fabricated from pristine cellulose using click chemistry reaction. PANI-NCC has endowed excellent sorption performance for Cr(III) and Cr(VI), respectively, owing to electrostatic interactions, mainly hard–hard interactions between chromium ions and amine functionalities present on the surface of PANI-NCC. The chemisorption, spontaneous, feasible, and exothermic nature of sorption process was ascertained

by equilibrium, kinetic, and thermodynamic parameters. The maximum sorption performances of Cr(III) and Cr(VI) were 47.06 and 48.92 mg g^{-1}. The sorption performance of Cr(VI) was higher than that of Cr(III) on account of low energy barrier of Cr(VI). In addition, the resulting sorbent was effectively applied to real industrial at optimum conditions. The PANI-NCC was reused for the recovery of chromium for 6 cycles. In the finale, this work addresses expertise of fabricated PANI-NCC for both forms of chromium together with beautiness such as reusability, aptitude in competitive environment, and specificity making them promising rival for water purification.

Acknowledgments Authors are thankful to Prof. P.K. Kalra, Director, Dayalbagh Educational Institute, Agra and Prof. Sahab Dass, Head of the Department, for extending all the necessary facilities and motivation to carry out the research. The financial support for this investigation given by Department of Science and Technology (DST), New Delhi, India under the grant DST/INSPIRE Fellowship/2014/IF140213 is gratefully acknowledged.

References

Akhavan B, Jarvis K, Majewski P (2015) Plasma polymer-functionalized silica particles for heavy metals removal. ACS Appl Mater Interfaces 7:4265–4274. doi:10.1021/am508637k

Anirudhan TS, Rejeena SR (2012) Poly(acrylicacid)-modified poly(glycidylmethacrylate)-grafted nanocellulose as matrices for adsorption of lysozyme from aqueous solutions. Chem Eng J 187:150–159. doi:10.1016/j.cej.2012.01.113

Anirudhan TS, Nima J, Divya PL (2013) Adsorption of chromium (VI) from aqueous solutions by glycidylmethacrylate-grafted-densified cellulose with quaternary ammonium groups. Appl Surf Sci 279:441–449. doi:10.1016/j.apsusc.2013.04.134

Asem AA, Ahied DM, Ahmed YM (2008) Removal of some hazardous heavy metals from aqueous solution using magnetic chelating resin with iminodiacetate functionality. Sep Purif Technol 61:348–357. doi:10.1016/j.seppur.2007.11.008

Benkaddour A, Jradi K, Robert S, Daneault C (2013) Grafting of polycaprolactone on oxidized nanocelluloses by click chemistry. Nanomaterials 3:141–157. doi:10.3390/nano3010141

Chingombe P, Saha B, Wakeman RJ (2005) Surface modification and characterization of a coal-based activated carbon. Carbon 43:3132–3143. doi:10.1016/j.carbon.2005.06.021

Cruz CCV, Da Costa ACA, Henriques ASL (2004) Kinetic modeling and equilibrium studies during cadmium biosorption by dead *Sargassum* sp. Biomass Bioresour Technol 91:249–257. doi:10.1016/S0960-8524(03)00194-9

Dhawan R, Bhasin KK, Goyal M (2015) Isotherms, kinetics and thermodynamics for adsorption of pyridine vapors on modified activated carbons. Adsorption 21:37–52. doi:10.1007/s10450-015-9648-x

Dichiara AB, Webber MR, Gorman WR, Rogers RE (2015) Removal of copper ions from aqueous solutions via adsorption on carbon nanocomposites. ACS Appl Mater Interfaces 7:15674–15680. doi:10.1021/acsami.5b04974

Donia AM, Atia AA, Abouzayed FI (2012) Preparation and characterization of nano-magnetic cellulose with fast kinetic properties towards the adsorption of some metal ions. Chem Eng J 191:22–25. doi:10.1016/j.cej.2011.08.034

Elwakeel K (2009) Removal of Mo(VI) as oxoanions from aqueous solutions using chemically modified magnetic chitosan resins. Hydrometallurgy 97:21–28. doi:10.1016/j.hydromet.2008.12.009

Espinosa SC, Kuhnt T, Foster EJ, Weder C (2013) Isolation of thermally stable cellulose nanocrystals by phosphoric acid hydrolysis. Biomacromolecules 14:1223–1230. doi:10.1021/bm400219u

Filpponen I, Kontturi E, Nummelin S, Rosilo H, Kolehmainen E, Ikkala O, Janne Laine J (2012) Generic method for modular surface modification of cellulosic materials in aqueous medium by sequential "click" reaction and adsorption. Biomacromolecules 13:736–742. doi:10.1021/bm201661k

Fumagalli M, Sanchez F, Molina-Boisseau S, Heux L (2015) Surface-restricted modification of nanocellulose aerogels in gas-phase esterification by di-functional fatty acid reagents. Cellulose 22:1451–1457. doi:10.1007/s10570-015-0585-3

Gardner DJ, Oporto GS, Mills R, Samir ASA (2008) Adhesion and surface issues in cellulose and nanocellulose. J Adhes Sci Technol 22:545–567. doi:10.1163/156856108X295509

Ghahafarrokhi IS, Khodaiyan F, Mousavi M, Yousefi H (2015) Preparation and characterization of nanocellulose from beer industrial residues using acid hydrolysis/ultrasound. Fibers Polym 16:529–536. doi:10.1007/s12221-015-0529-4

Gu X, Yang Y, Hu Y, Hu M, Wang C (2015) Fabrication of graphene-based xerogels for removal of heavy metal ions and capacitive deionization. ACS Sustain Chem Eng 3:1056–1065. doi:10.1021/acssuschemeng.5b00193

Gupta VK, Nayak A (2012) Cadmium removal and recovery from aqueous solutions by novel adsorbents prepared from orange peel and Fe_2O_3nanoparticles. Chem Eng J 180:81–90. doi:10.1016/j.cej.2011.11.006

Gupta VK, Srivastava SK, Mohan D, Sharma S (1998) Design parameters for fixed bed reactors of activated carbon developed from fertilizer waste for the removal of some heavy metal ions. Waste Manage 17:517–522. doi:10.1016/S0956-053X(97)10062-9

Gupta VK, Gupta M, Sharma S (2001) Process development for the removal of lead and chromium from aqueous solutions using red mud-an aluminium industry waste. Water Res 35:1125–1134. doi:10.1016/S0043-1354(00)00389-4

Gupta VK, Singh P, Rahman N (2004) Adsorption behavior of Hg(II), Pb(II) and Cd(II) from aqueous solution on Duolite C-433: a synthetic resin. J Colloid Interface Sci 275:398–402. doi:10.1016/j.jcis.2004.02.046

Gupta VK, Agarwal S, Saleh TA (2011a) Synthesis and characterization of alumina-coated carbon nanotubes and their application for lead removal. J Hazard Mater 185:17–23. doi:10.1016/j.jhazmat.2010.08.053

Gupta VK, Jain R, Nayak A, Agarwal S, Shrivastava M (2011b) Removal of the hazardous dye—tartrazine by photodegradation on titanium dioxide surface. Mater Sci Eng C 31:1062–1067. doi:10.1016/j.msec.2011.03.006

Gupta VK, Ali I, Saleh TA, Nayak A, Shilpi A (2012a) Chemical treatment technologies for waste-water recycling—an overview. RSC Adv 2:6380–6388. doi:10.1039/C2RA20340E

Gupta VK, Jain R, Mittal A, Saleh TA, Nayak A, Agarwal S, Sikarwar S (2012b) Photo-catalytic degradation of toxic dye

amaranth on TiO_2/UV in aqueous suspensions. Mater Sci Eng C 32:12–17. doi:10.1016/j.msec.2011.08.018

Gupta VK, Pathania D, Sharma S, Agarwal S, Singh P (2013) Remediation of noxious chromium (VI) utilizing acrylic acid grafted lignocellulosic adsorbent. J Mol Liq 177:343–352. doi:10.1016/j.molliq.2012.10.017

Gupta VK, Bhushan R, Nayak A, Singh P, Bhushan B (2014) Biosorption and reuse potential of a blue green alga for the removal of hazardous reactive dyes from aqueous solutions. Bioremedia J 18:179–191. doi:10.1080/10889868.2014.918574

Gurgel LVA, de Melo JCP, de Lena JC, Gil LF (2009) Adsorption of chromium(VI) ion from aqueous solution by succinylated mercerized cellulose functionalized with quaternary ammonium groups. Bioresour Technol 100:3214–3220. doi:10.1016/j.biortech.2009.01.068

Hokkanen S, Repo E, Sillanpaa M (2013) Removal of heavy metals from aqueous solutions by succinic anhydride modified mercerized nanocellulose. Chem Eng J 223:40–47. doi:10.1016/j.cej.2013.02.054

Jain AK, Gupta VK, Bhatanagar A, Suhas (2003) A comparative study of adsorbents prepared from industrial wastes for removal of dyes. Sep Sci Technol 38:463–481. doi:10.1081/SS-120016585

Kalidhasan S, Rajesh N (2009) Simple and selective extraction process for chromium(VI) in industrial wastewater. J Hazard Mater 170:1079–1085. doi:10.1016/j.jhazmat.2009.05.071

Kardam AK, Raj KR, Arora JK, Srivastava S (2012) Artificial neural network modelling for biosorption of Pb(II) ions on nanocellulose fibres. Bio Nano Sci 2:153–160. doi:10.1007/s12668-012-0045-6

Karthikeyan S, Gupta VK, Ramasamy B (2012) A new approach for the degradation of high concentration of aromatic amine by heterocatalytic Fenton oxidation: kinetic and spectroscopic studies. J Mol Liquids 173:153–163. doi:10.1016/j.molliq.2012.06.022

Khani H, Rofouei MK, Arab P, Gupta VK, Vafaei Z (2010) Multi-walled carbon nanotubes-ionic liquid-carbon paste electrode as a super selectivity sensor: application to potentiometric monitoring of mercury ion(II). J Hazard Mater 183:402–409. doi:10.1016/j.jhazmat.2010.07.039

Klemm D, Kramer F, Moritz S, Lindstrom T, Ankerfors M, Gray D, Dorris A (2011) Nanocelluloses: a new family of nature based materials. Angew Chem Int Ed 50:5438–5466. doi:10.1002/anie.201001273

Kumar ASK, Kalidhasan S, Rajesh V, Rajesh N (2012) Application of cellulose–clay composite biosorbent toward the effective adsorption and removal of chromium from industrial wastewater. Ind Eng Chem Res 51:58–69. doi:10.1021/ie201349h

Li Y, Zhu H, Xu M, Zhuang Z, Xu M, Dai H (2014) High yield preparation method of thermally stable cellulose nanowhiskers. Bioresources 9:1986–1997. doi:10.15376/biores.9.2.1986-1997

Lin N, Huang J, Dufresne A (2012) Preparation, properties and applications of polysaccharide nanocrystals in advanced functional nanomaterials: a review. Nanoscale 4:3274–3294. doi:10.1039/c2nr30260h

Liu M, Deng Y, Zhan H, Zhang X (2002) Adsorption and desorption of copper (II) from solutions on new spherical cellulose adsorbent. J Appl Polym Sci 84:478–485. doi:10.1002/app.10114

Lu P, Hsieh YL (2010) Preparation and properties of cellulose nanocrystals: rods, spheres, and network. Carbohydr Polym 82:329–336. doi:10.1016/j.carbpol.2010.04.073

Mittal A, Kaur D, Malviya A, Mittal J, Gupta VK (2009a) Adsorption studies on the removal of coloring agent phenol red from wastewater using waste materials as adsorbents. J Colloid Interface Sci 337:345–354. doi:10.1016/j.jcis.2009.05.016

Mittal A, Mittal J, Malviya A, Kaur D, Gupta VK (2009b) Adsorptive removal of hazardous anionic dye "Congo red" from wastewater using waste materials and recovery by desorption. J Colloid Interface Sci 340:16–26. doi:10.1016/j.jcis.2009.08.019

Mittal A, Mittal J, Malviya A, Kaur D, Gupta VK (2010a) Decoloration treatment of a hazardous triarylmethane dye, Light Green SF (Yellowish) by waste material adsorbents. J Colloid Interface Sci 342:518–527. doi:10.1016/j.jcis.2009.10.046

Mittal A, Mittal J, Malviya A, Gupta VK (2010b) Removal and recovery of Chrysoidine Y from aqueous solutions by waste materials. J Colloid Interface Sci 344:497–507. doi:10.1016/j.jcis.2010.01.007

Navarro JRG, Conzatti G, Yu Y, Fall AB, Mathew R, Edén M, Lennart Bergström L (2015) Multicolor fluorescent labeling of cellulose nanofibrils by click chemistry. Biomacromolecules 16:1293–1300. doi:10.1021/acs.biomac.5b00083

Qiu B, Guo J, Zhang X, Sun D, Gu H, Wang Q, Wang H, Wang X, Zhang XX, Weeks BL, Guo Z, Wei S (2014) Polyethylenimine facilitated ethyl cellulose for hexavalent chromium removal with a wide pH range. ACS Appl Mater Interfaces 6:19816–19824. doi:10.1021/am505170j

Qiu B, Gu H, Yan X, Guo J, Wang Y, Sun D, Wang Q, Khan M, Zhang X, Week BL, Young DP, Zhanhu G, Wei S (2015) Cr(VI) removal by magnetic carbon nanocomposites derived from cellulose at different carbonization temperatures. J Mater Chem A 2:17454–17462. doi:10.1039/C5TA01227A

Rahman N, Haseen U (2014) Equilibrium modeling, kinetic, and thermodynamic studies on adsorption of Pb(II) by a hybrid inorganic–organic material: polyacrylamide zirconium(IV) iodate. Ind Eng Chem Res 53:8198–8207. doi:10.1021/ie500139k

Renault F, Morin-Crini N, Gimbert F, Badot PM, Crini G (2008) Cationized starch-based material as a new ion-exchanger adsorbent for the removal of C.I. Acid Blue 25 from aqueous solutions. Bioresour Technol 99:7573–7586. doi:10.1016/j.biortech.2008.02.011

Saleh TA, Gupta VK (2012a) Column with CNT/magnesium oxide composite for lead(II) removal from water. Environ Sci Pollut Res 19:1224–1228. doi:10.1007/s11356-011-0670-6

Saleh TA, Gupta VK (2012b) Photo-catalyzed degradation of hazardous dye methyl orange by use of a composite catalyst consisting of multi-walled carbon nanotubes and titanium dioxide. J Colloid Interface Sci 371:101–106. doi:10.1016/j.jcis.2011.12.038

Shyaa AA, Hasan OA, Abbas AM (2015) Synthesis and characterization of polyaniline/zeolite nanocomposite for the removal of chromium(VI) from aqueous solution. J Saudi Chem Soc 19:101–107. doi:10.1016/j.jscs.2012.01.001

Singh K, Arora JK, Sinha TJM, Srivastava S (2014) Functionalization of nanocrystalline cellulose for decontamination of Cr(III) and Cr(VI) from aqueous system: computational modeling approach. Clean Technol Environ Policy 16:1179–1191. doi:10.1007/s10098-014-0717-8

Srivastava S, Kardam A, Raj KR (2012) Nanotech reinforcement onto cellulosic fibers: green remediation of toxic metals. Int J Green Nanotechnol 4:46–53. doi:10.1080/19430892.2012.654744

Tian Y, Wub M, Liu R, Li Y, Wang D, Tan J, Wu R, Huang Y (2011) Electrospun membrane of cellulose acetate for heavy metal ion adsorption in water treatment. Carbohydr Polym 83:743–748. doi:10.1016/j.carbpol.2010.08.054

Wang L, Zhang J, Zhao R, Li C, Li Y, Zhang C (2010) Adsorption of basic dyes on activated carbon prepared from *Polygonumorientale Linn*: equilibrium, kinetic and thermodynamic studies. Desalination 254:68–74. doi:10.1016/j.desal.2009.12.012

Wang L, Lu X, Lei S, Song Y (2014) Graphene-based polyaniline nanocomposites: preparation, properties and applications. J Mater Chem A 2:4491–4509. doi:10.1039/C3TA13462H

Wei H, Rodriguez K, Renneckar S, Vikesland P (2014) Environmental science and engineering applications of nanocellulose-based nanocomposites. Environ Sci Nano 1:302–316. doi:10.1039/C4EN00059E

Xue J, Song F, Yin X, Wang X, Wang Y (2015) Let it shine: a transparent and photoluminescent foldable nanocellulose/quantum dot paper. ACS Appl Mater Interfaces 7:10076–10079. doi:10.1021/acsami.5b02011

Yang J, Li L, Yan C (2011) Biosynthesis of spherical Fe_3O_4/bacterial cellulose nanocomposites as adsorbents for heavy metal ions. Carbohydr Polym 86:1558–1564. doi:10.1016/j.carbpol.2011.06.061

Zargoosh K, Abedini H, Abdolmaleki A, Molavian MR (2013) Effective removal of heavy metal ions from industrial wastes using thiosalicylhydrazide-modified magnetic nanoparticles. Ind Eng Chem Res 52:14944–14954. doi:10.1021/ie401971w

Zhang Y, Xu L, Zhao L, Peng J, Li C, Li J, Zhaia M (2012) Radiation synthesis and Cr(VI) removal of cellulose microsphere adsorbent. Carbohydr Polym 88:931–938. doi:10.1016/j.carbpol.2012.01.040